De Novo Molecular Design of Caspase-6 Inhibitors by GRU-Based Recurrent Neural Network Combined with Transfer Learning Approach

Shuheng Huang
Chongqing University https://orcid.org/0000-0001-8552-7319
Hu Mei (meihu@cqu.edu.cn)
Chongqing University https://orcid.org/0000-0001-5010-2978
Laichun Lu
Chongqing University https://orcid.org/0000-0002-9127-8678
Tingting Shi
Chongqing University https://orcid.org/0000-0001-6213-1784
Linxin Chen
Chongqing University https://orcid.org/0000-0003-0394-7251
Zuyin Kuang
Chongqing University https://orcid.org/0000-0002-0985-1421
Yu Heng
Chongqing University https://orcid.org/0000-0002-8419-5399
Lei Xu
Chongqing University https://orcid.org/0000-0002-9571-6129
Xianchao Pan
Southwest Medical University https://orcid.org/0000-0002-1269-683X

Research article

Keywords: gated recurrent unit, recurrent neural network, transfer learning, caspase-6, inhibitor, molecular design

Posted Date: April 20th, 2020

DOI: https://doi.org/10.21203/rs.3.rs-22726/v1

Abstract

Due to the potencies in the treatments of neurodegenerative diseases, caspase-6 inhibitors have attracted widespread attentions. Herein, gated recurrent unit (GRU)-based recurrent neural network (RNN) combined with transfer learning was used to build the molecular generative model of caspase-6 inhibitors. The results showed that the GRU-based RNN model can learn accurately the SMILES grammars of about 2.4 million chemical molecules including ionic and isomeric compounds, and can generate potential caspase-6 inhibitors after transfer learning of the known 433 caspase-6 inhibitors. Further exploration of the chemical space and molecular docking showed that the generated potential inhibitors have similar chemical space distributions and binding mechanisms with the known caspase-6 inhibitors. In addition, 3 potential caspase-6 inhibitors with nanomolar-level activities were obtained and proved to be the most promising candidates for the further researches. In general, this paper provides an efficient combinational strategy for de novo molecular design of caspase-6 inhibitors.

Introduction

Caspase is a family of cysteinyl aspartate-specific proteases, which plays a critical role in the cell regulatory networks controlling inflammation and programmed cell death.[1] Up to now, 11 functional caspase subtypes (i.e. caspase 1–10, 14) have been found in human encode proteins, of which caspase-1, -4 and − 5 are related to inflammatory response, caspase-14 to keratinocyte differentiation and others to apoptosis. The apoptotic caspases are further divided into two subcategories, namely apoptotic initiator and executioner caspases according to their functions in apoptosis processes. The initiator caspases (caspases-2, -8, -9, and − 10) can be recruited and activated by either death receptors or apoptosomes, while the downstream executioner caspases (caspases-3, -6, and − 7) are responsible for the actual cell destruction.[2–4]

Accumulated evidences have suggested that the activation of caspase-6 is responsible for neuronal apoptosis and amyloid β peptide (Aβ) deposition, which is highly involved in age-dependent axon degeneration and neurodegenerative diseases, such as Huntington's disease and Alzheimer's disease.[5–7] Due to the potencies in the treatments of neurodegenerative diseases, caspase-6 inhibitors have attracted intensive attentions. Recently, a series of aza-peptides,[8] acyl dipeptides,[9, 10] and non-peptide benzenesulfonyl chloride, isatin sulfonamide,[11–15] tetrafluorophenoxy methyl ketone,[16] phenothiazin-5-ium derivatives,[17] heteroaryl propanamido hexanoic acid,[18] vinyl sulfone,[19] furoyl-phenylalanine derivatives[20] have been identified as caspase-6 inhibitors with nanomolar to micromolar potencies (Fig. 1). In spite of promising efficacies, the available caspase-6 inhibitors also showed inevitable pharmacokinetic deficiencies (e.g. cell toxicity, low permeability, metabolic instability) that restrict their clinical applications.[21]

Over the last decade, deep learning (DL) technologies, such as convolutional networks (CNN), restricted Boltzmann machine (RBM), recurrent neural networks (RNN), and generative adversarial network (GAN) have been gradually applied in drug design and proven to be promising approaches for artificial

intelligence-based drug design.[22], [23, 24] Recently, RNN-based molecular generative network has attracted particular attentions duo to its unique features in *de novo* molecular design.

In this paper, gated recurrent unit (GRU)-based RNN network combined with transfer learning and traditional machine learning were employed for *de novo* molecular design of caspase-6 inhibitors. The results showed that the established generative RNN model can generate efficiently potent caspase-6 inhibitors with the similar chemical space distribution to the known caspase-6 inhibitors, which can be easily incorporated with the traditional molecular design methods. Collectively, this paper provides an efficient combinational strategy for *de novo* molecular design of caspase-6 inhibitors.

Methods

Datasets

In this paper, about 2.4 million chemical molecules including ionic and isomeric compounds were firstly retrieved from PubChem database. Then, all of the known caspase-6 inhibitors were removed from the dataset. In order to decrease the degree of data heterogeneity, only the molecules with the number of heavy atoms between 10 and 100 and the length of canonical SMILES string less than 140 were selected. As a result, a total of 2,393,029 molecules (SMILES strings) were retained for training the generative RNN network.

To construct a prediction model of caspase-6 inhibitors, 1656 samples consisting of 577 caspase-6 inhibitors and 1079 non-inhibitors were derived from the recent literatures (Table S1 and S2).[9–15, 25–35] The activities of the collected caspase-6 inhibitors were mainly detected by enzyme inhibition assays and fluorescent plate reader assay.

Machine learning based classification models of caspase-6 inhibitors

Firstly, the 577 caspase-6 inhibitors and 1079 non-inhibitors were divided into a training/validation set (433 positives/579 negatives) and a test set (144 positives/500 negatives) according to Table S1. Then, the positive and negative samples in the training/validation set were further randomly divided into the training and validation sets at a ratio of 6:4, respectively. The statistic information of the datasets refers to Table S2. Lastly, a total of 200 fragmental and topological descriptors (Table S3) generated by RDKit toolkit were used for the structural description of the 1656 samples. Herein, five machine learning methods, i.e., support vector machine (SVM), k-nearest neighbor (KNN), Gaussian Naïve Bayesian (GNB), random forest (RF) and logistic regression (LR), were used to construct binary classification models by Scikit-Learn toolkit.[36] The ROC (receiver operating characteristic), AUC (area under curve), Matthews correlation coefficient (MCC), accuracy (Acc), specificity (Spe) and sensitivity (Sen) were used for model evaluations.

Generative RNN modeling and transfer learning

The architecture of the generative RNN model is composed of one input layer, one auto-embedding layer with 128 dimensions, three GRU layers with 512 neurons in each layer, and one output layer with softmax activation function (Fig. 3). The input layer is responsible for receiving the sequential tokens of the SMILES string of a given sample and the output layer for calculating the occurrence probability of the token at the next position. In this paper, the RNN network was trained by Adam optimizer,[37] of which the initial learning rate is set to 0.001 with a decay rate of 0.05 every 300 steps. The batch size was set to 128 and the loss function was defined as negative log likelihood function. After pretrained by the 2,393,029 SMILES strings from PubChem database, the RNN network was further fine-turned by using the 433 caspase-6 inhibitors in the training and validation datasets.

Molecular docking

Surflex-dock (Sybyl 8.1, Tripos Inc)[38] has been proved be an efficient receptor-based drug design and virtual screening strategy, which employs a protomol to guide the generation process of putative ligand binding poses. Herein, a crystal structure of caspase-6 (PDB ID: 3OD5) was used for generating the protomol based on the residues within the 8 Å distance to the co-crystallized ligand Ac-VEID-CHO. Before docking, the structures of the ligands were charged by MMFF94 method and then optimized by Tripos force field with conjugate gradient minimizer. The maximum iteration steps and energy gradient were set to 10000 times and 0.05 kcal/mol·Å. To promote the precision of the docking procedure, 3 additional starting conformations per ligand, self-scoring, ring flexibility, soft grid, pre- and post-dock minimizations were also considered in this paper.

Results And Discussion

Performances of ML predictors

Table 1
The prediction performances on the 644 test samples by the optimal LR model

	Confusion matrix			Performance			
		PP	PN	Acc	Spe	Sen	MCC
Independent test set	TP	102	42	0.86	0.90	0.71	0.60
	TN	49	451				

PP: predicted positive; PN: predicted negative; TP: true positive; TN: true negative.

The generative RNN modeling

Herein, 2393029 SMILES strings derived from Pubchem database were used for pre-training the RNN models. Firstly, the effect of the number of GRU layers on the performance of the generative RNN model was investigated based on the network architecture shown in Fig. 3. It can be seen that, after 14000 steps of iterations, the loss values of the RNN models with one, two and three GRU layers reach the state of

convergence (Fig. 5a). At the mean time, the valid percentages of 128 SMILES strings sampled by the 3 RNN models reach to 0.85, 0.90 and 0.95, respectively. Besides, no significant improvement in the valid percentage was observed for the RNN models with more than 3 GRU layers. Thus, the RNN model with 3 GRU layers was chosen for the following transfer learning.

In this paper, the 433 caspase-6 inhibitors in the training and validation sets (Table S2) were used for the transfer learning of the pre-trained RNN model. From Fig. 5b, it can be observed that, after 200 steps of fine-tuning, the loss value tends to converge and the valid percentage of the sampled SMILES strings reached to 99%.

In order to evaluate the performance of the refined RNN model in generating potential caspase-6 inhibitors, a retrospective study was performed by using the 144 caspase-6 inhibitors in the test dataset (Table S2), which the RNN model had never seen before. At first, a total of 50,000 valid SMILES strings were randomly sampled by the fine-tuned RNN model. After structural description by using RDKit toolkit, the 50,000 molecules were then predicted by the LR predictor. Based on the predicted positive samples, the recall rate of the 144 caspase-6 inhibitors was finally calculated. As shown in Table 2, it can be seen that the percentage of the predicted positive samples maintains at a relatively high level during the whole sampling process. Also, it can be noticed that the recall rate of the 144 caspase-6 inhibitors increases gradually from the lowest value of 2.08% to the highest value of 13.19% (Table 2). Accordingly, it can be concluded that the RNN model can generate efficiently the potential caspase-6 inhibitors after transfer learning. It should be noted that the relatively low recall rate is mainly caused by the small sample size of the test caspase-6 inhibitors.

Table 2
The recall rates of the 144 caspase-6 inhibitors

Sampling Process	I	II	III	IV	V	VI	VII	VIII	IX	X
No. of SMILES strings	1000	2000	3000	4000	5000	10000	20000	30000	40000	50000
The predicted positive samples (%)	76.0	72.7	71.4	70.7	70.6	69.3	67.1	66.2	65.5	65.0
Recall rate (%)	2.08	2.08	3.47	5.55	6.94	8.33	10.41	11.80	13.19	13.19

The distribution in chemical space of the potential caspase-6 inhibitors

According to Table 2, a total of 6927 strings (69.3%) were predicted as positive samples from the 10,000 SMILES strings generated. Herein, based on the properties of H-Bond acceptor/donor, rotatable bonds,

aromatic/aliphatic cycles, heterocycle atoms and molecular weight, the distribution of the potential 6927 caspase-6 inhibitors was explored by using t-distributed stochastic neighbor embedding (t-SNE) method.

From Fig. 6, it can be inferred that the generated 6927 potential inhibitors have the similar chemical space as the known 577 caspase-6 inhibitors. Herein, three small clusters of the samples were selected to explore the structural features in detail. For each cluster, it can be observed that the generated molecules have similar molecular scaffolds with the known caspase-6 inhibitors (Fig. 6). The structural modification mainly involves substituent modification, scaffold hopping, and chiral transformation etc., which are also the major means in traditional drug design.

Molecular docking-based ligand screening

Before docking-based screening of the caspase-6 inhibitors, the protocol of Surflex-dock was firstly validated by re-docking a co-crystallized ligand Ac-VEID-CHO into the binding pocket of caspase-6 (PDB: 3OD5). The results showed that Surflex-dock can reproduce the native ligand binding conformation with a docking score of 7.67 (Figure S1).

Based on the docking results of the 577 known caspase-6 inhibitors and the potential 6927 positive samples, the occurrence frequencies of the residues involved in the intermolecular interactions with the 577 caspase-6 inhibitors and 6927 potential inhibitors were investigated respectively. From Fig. 7a, it can be clearly seen that the distributions in the occurrence frequencies of the binding residues are quite similar between the two cases, especially for the binding residues with the occurrence frequencies larger than 50%. Therefore, it can be deduced that the potential 6927 inhibitors have similar binding mode with the known 577 caspase-6 inhibitors.

Herein, three representative positive samples (ID: 96, 2470 and 3262) with different scaffolds were further investigated. The docking scores of the 3 positive samples are higher than 9.0 (-logKD), which indicates strong inhibitory activities at nanomolar level. As shown in Fig. 7b, both of the sample 96 and 2470 can form strong H-bond interactions with Arg220, while sample 3262 form 3 H-bonds with Arg64, His121 and Gln161. For sample 2470 and 3262, strong π-cation interactions with Arg220 can be also observed. Recent researches have proved that Arg64, Gln161, and Arg220 are closely related with the substrate-specificity of caspase-6, and that His121 is a key catalytic residue for substrate hydrolysis [1]. Besides, all the 3 samples can form strong hydrophobic interactions with the hotspot residue Tyr217, Val261, Cys264 and Ala269. Collectively, the 3 potential caspase-6 inhibitors with nanomolar-level activities are promising candidates for the further researches.

Conclusions

In this paper, GRU-based RNN network combined with transfer learning was employed for *de novo* molecular design of caspase-6 inhibitors. The results showed that the established GRU-based RNN model can learn accurately the SMILES grammars of 2.4 million chemical molecules including ionic and isomeric compounds and be capable of generating novel potent caspase-6 inhibitors after transfer

learning of the known 433 caspase-6 inhibitors. According to the distributions in the chemical space of the generated positive samples with the known inhibitors, it can be inferred that the fine-tuned RNN model can generate the potential target molecules with similar chemical space to the known caspase-6 inhibitors. Further analysis showed that the novel caspase-6 inhibitors can be generated by substituent modification, scaffold hopping, and chiral transformation etc. operations on the level of SMILES stings. Based on the docking results, 3 representative inhibitors with high docking scores were investigated and proved to be the most promising candidates. In general, the framework presented in this paper provides an efficient combinational strategy for *de novo* molecular design of caspase-6 inhibitors.

Declarations

Acknowledgements

Not applicable.

Authors' contributions

Formal analysis, S.H.; Funding acquisition, H.M., X.P. and S.H.; Methodology, L.C. and T.S.; Resources, S.H., Z.K., Y.H. and L.X.; Writing-original draft, S.H.; Writing-review & editing, L.L., H.M. and X.P. All authors have read and agreed to the published version of the manuscript.

Funding

The authors acknowledge the support of Fundamental Research Funds for the Central Universities (Project No.106112017CDJQJ238816), Collaborative Fund of Science and Technology Agency of Luzhou Government and Southwest Medical University (Project No.2019LZXNYDZ05) and Graduate Scientific Research and Innovation Foundation of Chongqing (Project No. CYB19042).

Availability of data and materials

Code, data, and pre-trained models are available from GitHub (https://github.com/ShuhengH/De-Novo-Caspase-6-Inhibitors-Design-by-GRU-Based-RNN-Combined-with-Transfer-Learning-Approach).

Competing interests

The authors declare that they have no competing interests.

References

1. Clark AC (2016) Caspase Allostery and Conformational Selection. Chem Rev 116(11):6666–6706
2. Slee EA, Adrain C, Martin SJ (2001) Executioner caspase-3,-6, and-7 perform distinct, non-redundant roles during the demolition phase of apoptosis. J Biol Chem 276(10):7320–7326

3. McIlwain DR, Berger T, Mak TW (2013) Caspase functions in cell death and disease. Cold Spring Harb Perspect Biol 5(4):a008656
4. Denecker G, Ovaere P, Vandenabeele P et al (2008) Caspase-14 reveals its secrets. J Cell Biol 180(3):451–458
5. Wang XJ, Cao Q, Zhang Y et al (2015) Activation and Regulation of Caspase-6 and Its Role in Neurodegenerative Diseases. Annu Rev Pharmacol Toxicol 55:553–572
6. LeBlanc A, Liu H, Goodyer C et al (1999) Caspase-6 role in apoptosis of human neurons, amyloidogenesis, and Alzheimer's disease. J Biol Chem 274(33):23426–23436
7. Klaiman G, Petzke TL, Hammond J et al (2008) Targets of Caspase-6 activity in human neurons and Alzheimer disease. Mol Cell Proteomics 7(8):1541–1555
8. Sexton KB, Kato D, Berger AB et al (2007) Specificity of aza-peptide electrophile activity-based probes of caspases. Cell Death Differ 14(4):727–732
9. Linton SD, Karanewsky DS, Ternansky RJ et al (2002) Acyl Dipeptides as reversible caspase inhibitors. Part 1: Initial lead optimization. Bioorg Med Chem Lett 12(20):2969–2971
10. Linton SD, Karanewsky DS, Ternansky RJ et al (2002) Acyl Dipeptides as reversible caspase inhibitors. Part 2: Further optimization. Bioorg Med Chem Lett 12(20):2973–2975
11. Chu WH, Rothfuss J, d'Avignon A et al (2007) Isatin sulfonamide analogs containing a michael addition acceptor: A new class of caspase 3/7 inhibitors. J Med Chem 50(15):3751–3755
12. Chu WH, Rothfuss J, Chu YX et al (2009) Synthesis and in Vitro Evaluation of Sulfonamide Isatin Michael Acceptors as Small Molecule Inhibitors of Caspase-6. J Med Chem 52(8):2188–2191
13. Chu WH, Rothfuss J, Zhou D et al (2011) Synthesis and evaluation of isatin analogs as caspase-3 inhibitors: Introduction of a hydrophilic group increases potency in a whole cell assay. Bioorg Med Chem Lett 21(8):2192–2197
14. Limpachayaporn P, Schafers M, Schober O et al (2013) Synthesis of new fluorinated, 2-substituted 5-pyrrolidinylsulfonyl isatin derivatives as caspase-3 and caspase-7 inhibitors: Nonradioactive counterparts of putative PET-compatible apoptosis imaging agents. Bioorg Med Chem 21(7):2025–2036
15. Limpachayaporn P, Wagner S, Kopka K et al (2014) Synthesis of 7-Halogenated Isatin Sulfonamides: Nonradioactive Counterparts of Caspase-3/-7 Inhibitor-Based Potential Radiopharmaceuticals for Molecular Imaging of Apoptosis. J Med Chem 57(22):9383–9395
16. Leyva MJ, Degiacomo F, Kaltenbach LS et al (2010) Identification and evaluation of small molecule pan-caspase inhibitors in Huntington's disease models. Chem Biol 17(11):1189–1200
17. Pakavathkumar P, Sharma G, Kaushal V et al (2015) Methylene Blue Inhibits Caspases by Oxidation of the Catalytic Cysteine. Sci Rep 5
18. Lee H, Shin EA, Lee JH et al (2018) Caspase inhibitors: a review of recently patented compounds (2013–2015). Expert Opin Ther Pat 28(1):47–59

19. Pakavathkumar P, Noel A, Lecrux C et al (2017) Caspase vinyl sulfone small molecule inhibitors prevent axonal degeneration in human neurons and reverse cognitive impairment in Caspase-6-overexpressing mice. Mol Neurodegener 12
20. Heise CE, Murray J, Augustyn KE et al (2012) Mechanistic and Structural Understanding of Uncompetitive Inhibitors of Caspase-6. PLoS One 7(12)
21. MacKenzie SH, Schipper JL, Clark AC (2010) The potential for caspases in drug discovery. Curr Opin Drug Disc 13(5):568–576
22. Sellwood MA, Ahmed M, Segler MHS et al (2018) Artificial intelligence in drug discovery. Future Med Chem 10(17):2025–2028
23. Jing Y, Bian Y, Hu Z et al (2018) Deep Learning for Drug Design: an Artificial Intelligence Paradigm for Drug Discovery in the Big Data Era. AAPS J 20(3):58
24. Gawehn E, Hiss JA, Schneider G (2016) Deep Learning in Drug Discovery. Mol Inform 35(1):3–14
25. Wang Y, Huang JC, Zhou ZL et al (2004) Dipeptidyl aspartyl fluoromethylketones as potent caspase-3 inhibitors: SAR of the P-2 amino acid. Bioorg Med Chem Lett 14(5):1269–1272
26. Choong IC, Lew W, Lee D et al (2002) Identification of potent and selective small-molecule inhibitors of caspase-3 through the use of extended tethering and structure-based drug design. J Med Chem 45(23):5005–5022
27. Asgian JL, James KE, Li ZZ et al (2002) Aza-peptide epoxides: A new class of inhibitors selective for clan CD cysteine proteases. J Med Chem 45(23):4958–4960
28. Lee D, Long SA, Murray JH et al (2001) Potent and selective nonpeptide inhibitors of caspases 3 and 7. J Med Chem 44(12):2015–2026
29. Wang Y, Guan LF, Jia SJ et al (2005) Dipeptidyl aspartyl fluoromethylketones as potent caspase inhibitors: peptidomimetic replacement of the P-2 alpha-amino acid by a alpha-hydroxy acid. Bioorg Med Chem Lett 15(5):1379–1383
30. Han YX, Giroux A, Colucci J et al (2005) Novel pyrazinone mono-amides as potent and reversible caspase-3 inhibitors. Bioorg Med Chem Lett 15(4):1173–1180
31. Wang Y, Jia SJ, Tseng B et al (2007) Dipeptidyl aspartyl fluoromethylketones as potent caspase inhibitors: Peptidomimetic replacement of the P-2 amino acid by 2-aminoaryl acids and other non-natural amino acids. Bioorg Med Chem Lett 17(22):6178–6182
32. Thompson CM, Quinn CA, Hergenrother PJ (2009) Total Synthesis and Cytoprotective Properties of Dykellic Acid. J Med Chem 52(1):117–125
33. Mott BT, Ferreira RS, Simeonov A et al (2010) Identification and Optimization of Inhibitors of Trypanosomal Cysteine Proteases: Cruzain, Rhodesain, and TbCatB. J Med Chem 53(1):52–60
34. Rosse G (2013) Irreversible Inhibitors of Cysteine Proteases. ACS Med Chem Lett 4(2):163–164
35. Krause-Heuer AM, Howell NR, Matesic L et al (2013) A new class of fluorinated 5-pyrrolidinylsulfonyl isatin caspase inhibitors for PET imaging of apoptosis. Medchemcomm 4(2):347–352

36. Pedregosa F, Varoquaux G, Gramfort A et al (2011) Scikit-learn: Machine Learning in Python. J Mach Learn Res 12:2825–2830
37. Kingma D, Ba J (2014) Adam: a method for stochastic optimization. arXiv:14126980
38. Jain AN (2003) Surflex: Fully automatic flexible molecular docking using a molecular similarity-based search engine. J Med Chem 46(4):499–511

Figures

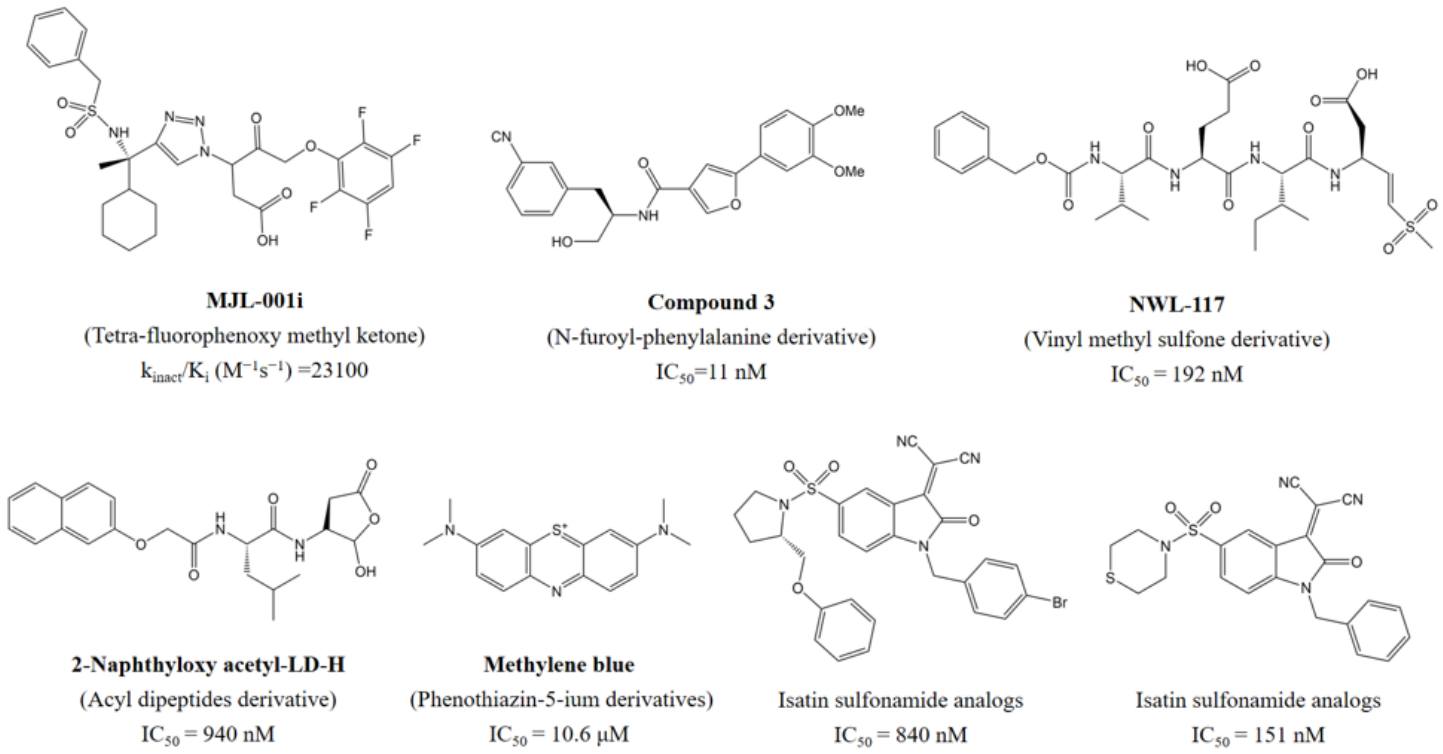

Figure 1

Representative structures of caspase-6 inhibitors.

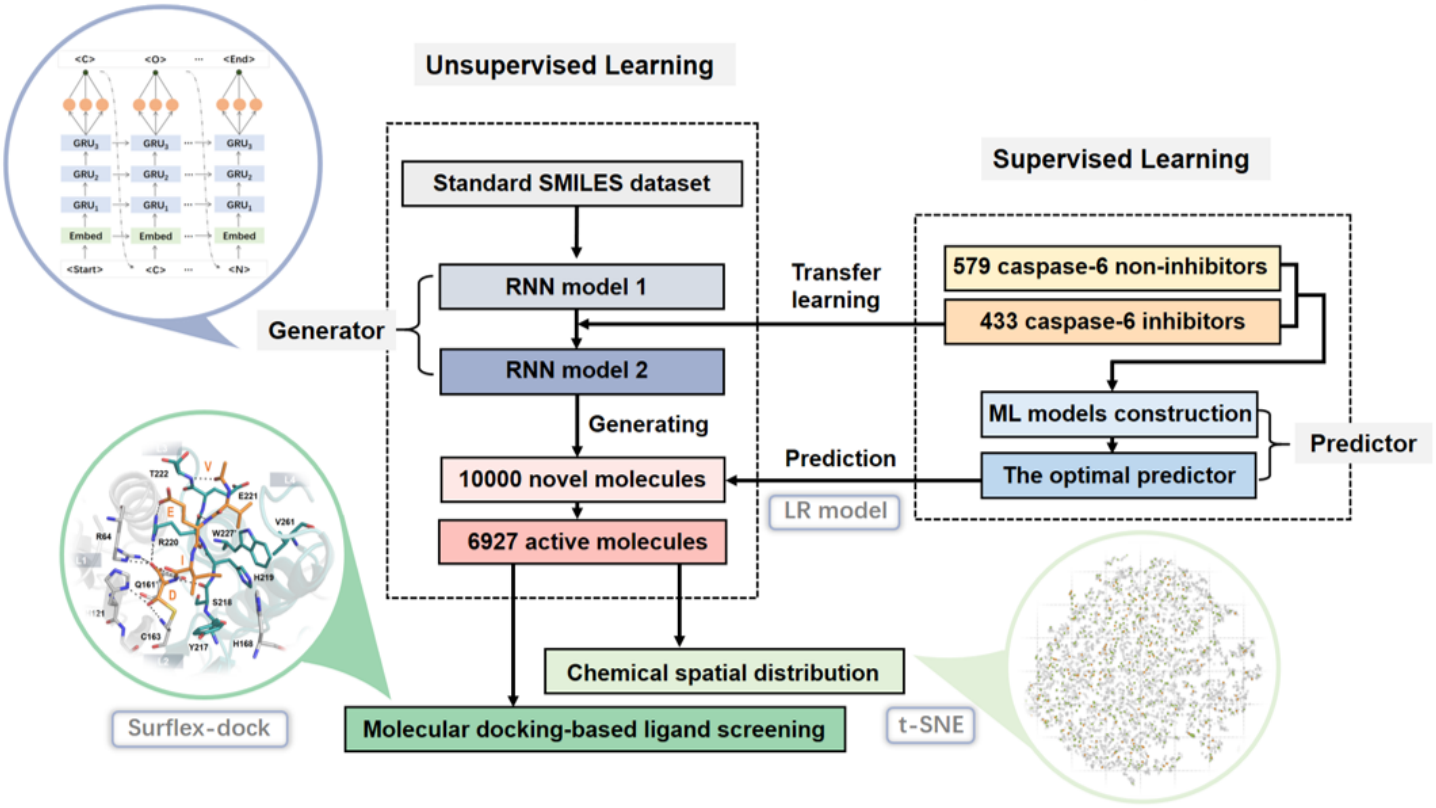

Figure 2

The flowchart of de novo molecular design of the caspase-6 inhibitors.

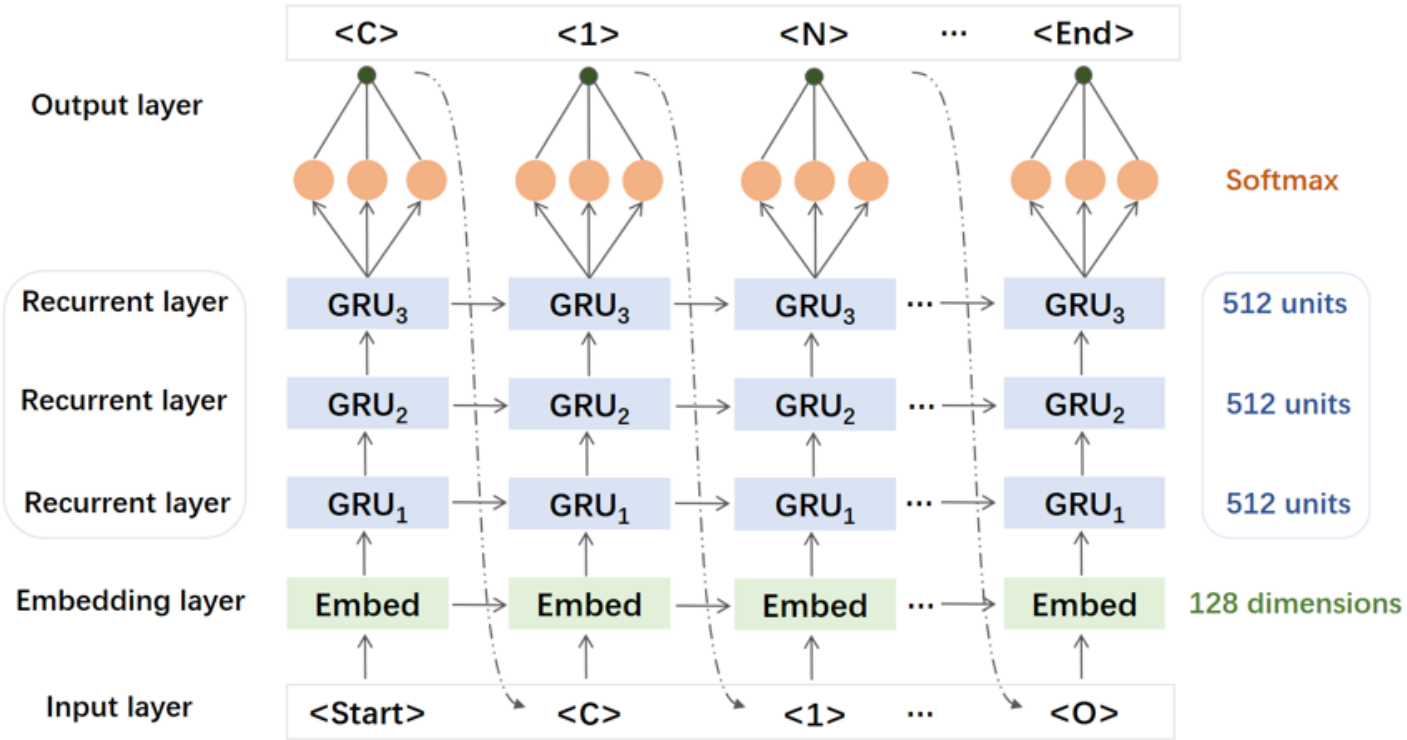

Figure 3

The architecture of the GRU-based recurrent neural network

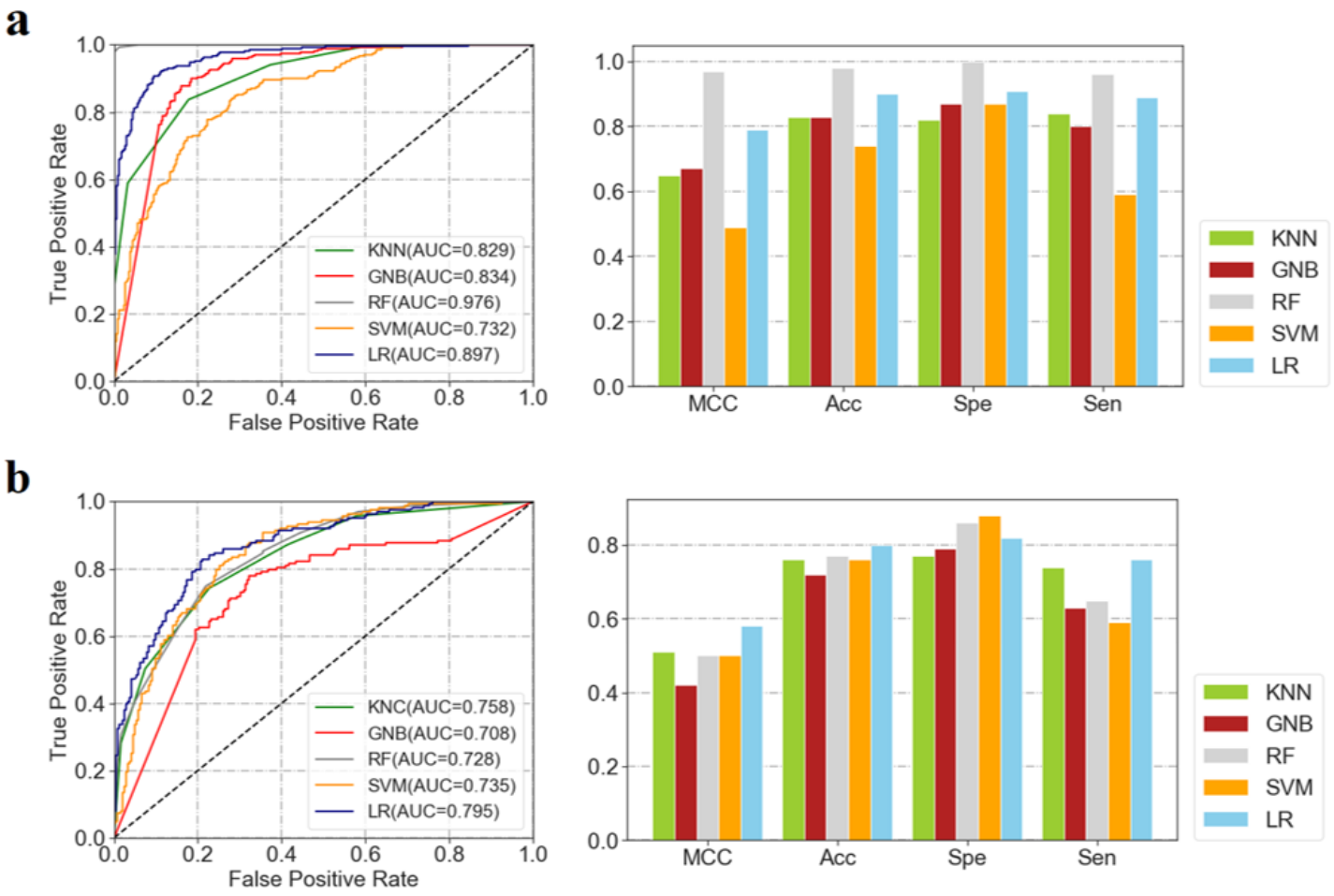

Figure 4

The performances of the 5 ML models on the training (a) and validation dataset (b). (SVM model: a radial basis function (RBF) kernel was used, of which the C and γ were set as 1 and 'auto', respectively; LR model: the inverse of regularization strength, tolerance for stopping criteria, maximum number of iterations, and penalty were set as 0.5, 0.001, 200, and "L1" respectively. Herein, default parameters were used for the ML models if not specified.)

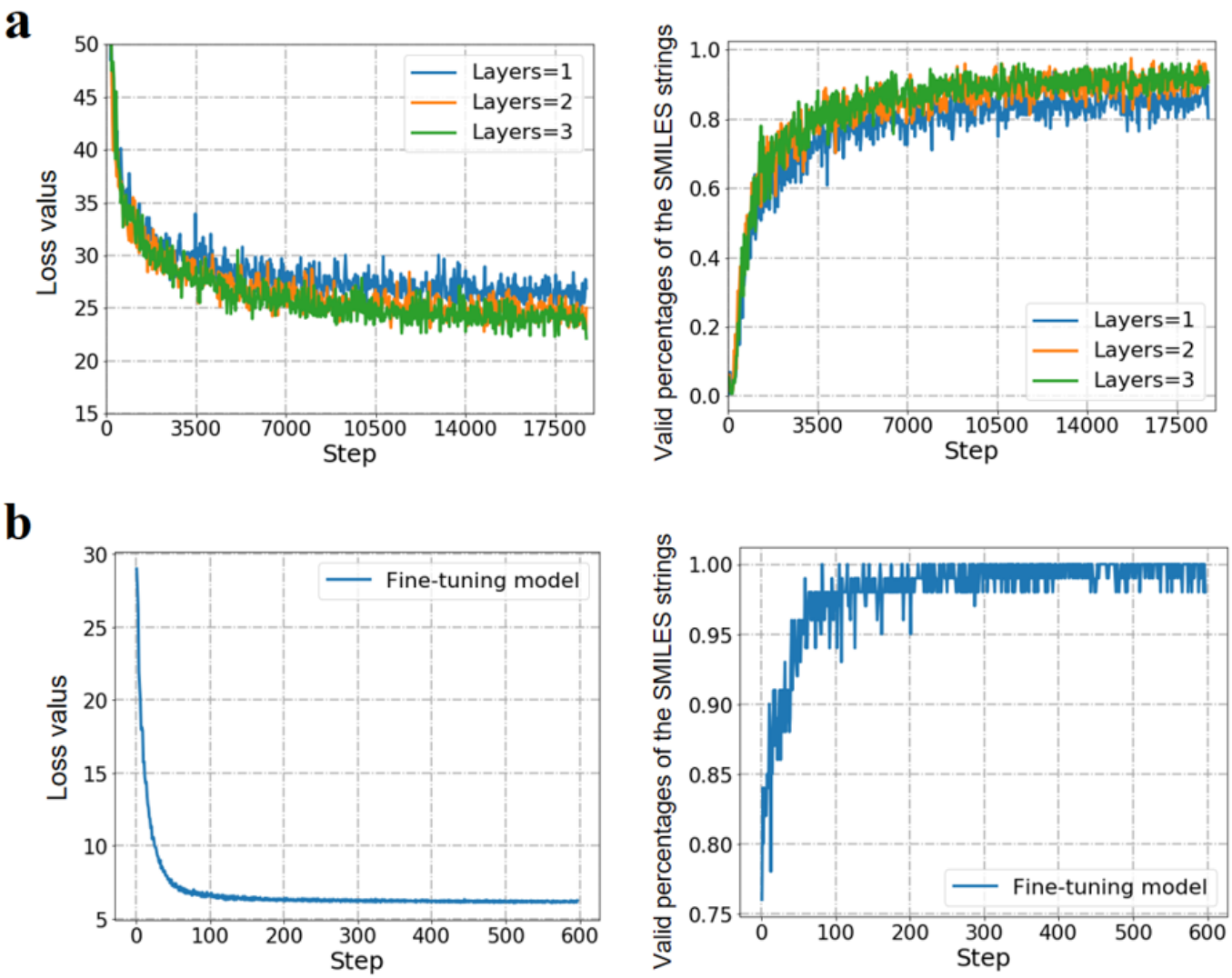

Figure 5

Performances of the pre-trained RNN models with different GRU layers (a) and the fine-tuned RNN model by transferred learning of 433 caspase-6 inhibitors (b)

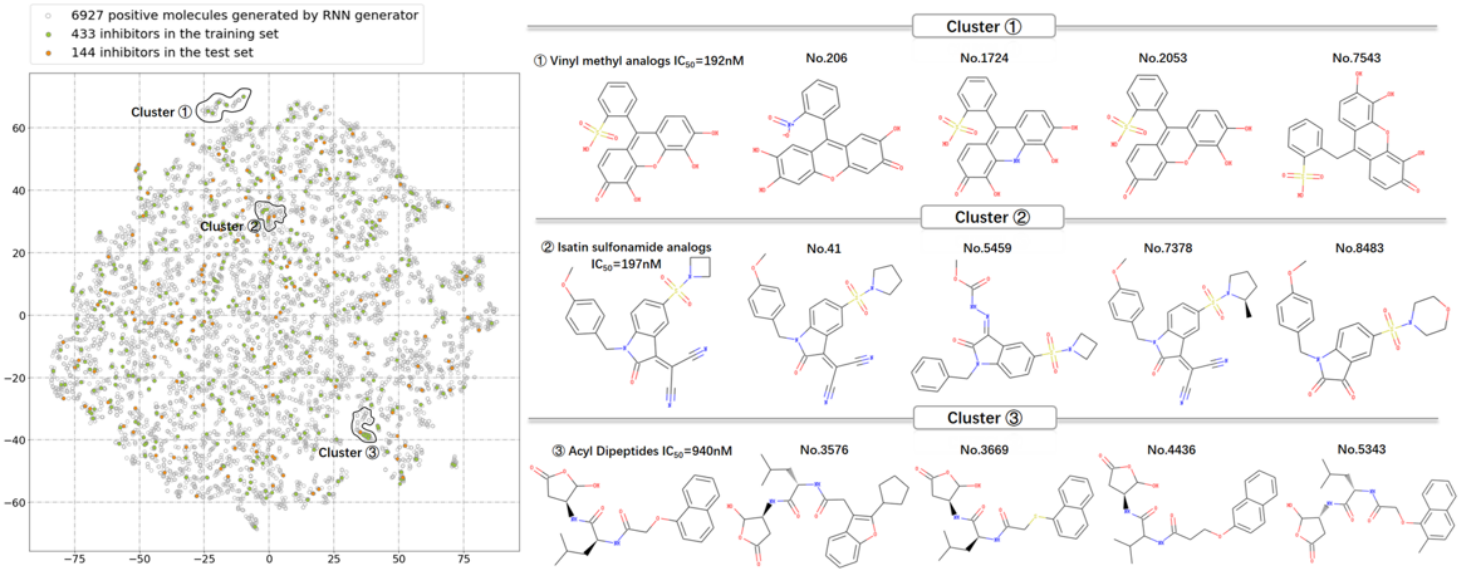

Figure 6

The distribution in the chemical space of the 6927 generated molecules (grey) and 577 known caspase-6 inhibitors (green: training samples; yellow: test samples)

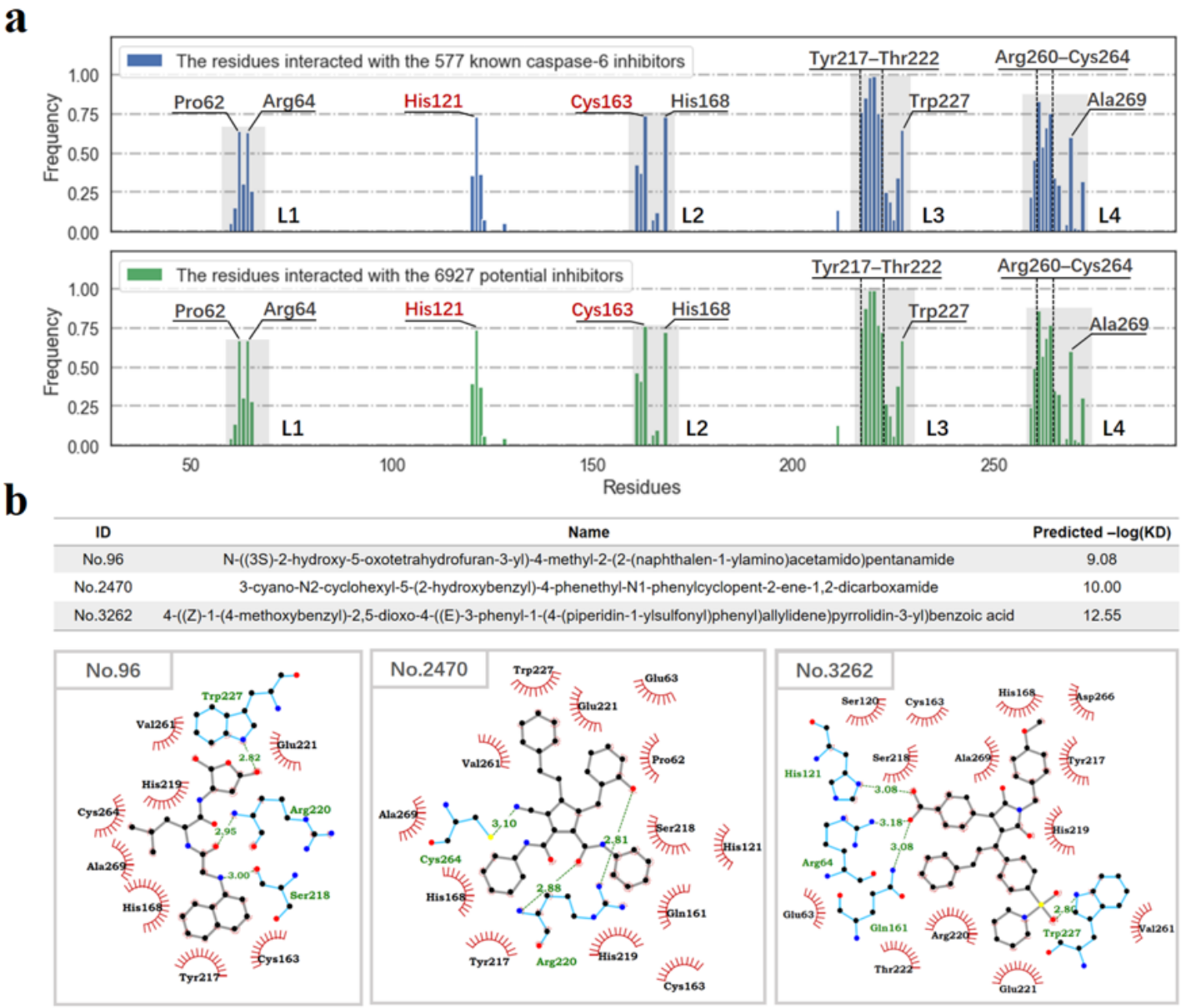

ID	Name	Predicted –log(KD)
No.96	N-((3S)-2-hydroxy-5-oxotetrahydrofuran-3-yl)-4-methyl-2-(2-(naphthalen-1-ylamino)acetamido)pentanamide	9.08
No.2470	3-cyano-N2-cyclohexyl-5-(2-hydroxybenzyl)-4-phenethyl-N1-phenylcyclopent-2-ene-1,2-dicarboxamide	10.00
No.3262	4-((Z)-1-(4-methoxybenzyl)-2,5-dioxo-4-((E)-3-phenyl-1-(4-(piperidin-1-ylsulfonyl)phenyl)allylidene)pyrrolidin-3-yl)benzoic acid	12.55

Figure 7

The binding modes of the 577 known caspase-6 inhibitors and 6927 potential inhibitors. (a) The occurrence frequencies of the binding residues involved in the intermolecular interactions with the binding ligands (The distance cutoff was set to 5 Å). The residues with the occurrence frequencies larger than 50% are marked, and the catalytic dyad residues His121 and Cys163 are colored in red. (b) Schematic diagrams of protein-ligand interactions of three representative samples. H-bonds are represented as green dashed lines. The carbon, nitrogen, oxygen, sulfur atoms were colored in black, blue, red and yellow, respectively.

Supplementary Files

This is a list of supplementary files associated with this preprint. Click to download.

- SupplementaryMaterial.docx